jority of the experiments done on laterally diffused light could be redone: Hanle effect of odd isotopes, double resonance in weak or strong magnetic field, level crossing in strong field, and study of the true resonance levels (some results were recently obtained[14] on the 5^1P_1 level of Cd). We are continuing these experiments on the combined effect of multiple diffusion, collisions between mercury atoms, and collisions of excited atoms on the wall of the cell. On the other hand, the systematic study of the signals observed directly from the light emitted by a discharge lamp could give information on the radiative transfer in the lamp, resonant and nonresonant collisions and possibly information on the parameters associated with the discharge. It is certainly possible to appreciably improve the experimental setup to test in detail more elaborate theories which will eventually appear.

ACKNOWLEDGMENTS

One of the authors (B. D.) would like to express her gratitude to the University of New Hampshire for the hospitality extended during the writing of this paper.

---

[*] Present address: Physics Department, Wellesley College, Wellesley, Mass. 02181.

[1] B. Dodsworth and A. Omont, preceding paper, Phys. Rev. A 3, 1901 (1971).

[2] W. Hanle, Z. Physik 30, 93 (1924).

[3] M. A. Guiochon, J. E. Blamont, and J. Brossel, J. Phys. Radium 18, 99 (1957).

[4] J. P. Barrat, J. Phys. Radium 20, 541 (1959); 20, 633 (1959); 20, 657 (1959).

[5] C. G. Carrington and A. Corney, Opt. Commun. 1, 115 (1969), and references quoted in this paper.

[6] A. Omont, thesis, Paris, 1967 (unpublished).

[7] B. Cagnac, Ann. Phys. (Paris) 6, 467 (1961).

[8] B. Dodsworth and A. Omont, Compt. Rend. 267B, 396 (1968).

[9] B. Dodsworth, J. C. Gay, and A. Omont, J. Phys. (Paris) (to be published).

[10] The results obtained with an excitation beam parallel to $\vec{H}$ have already been published in Ref. 8.

[11] M. I. Dyakonov and V. I. Perel, Zh. Eksperim. i Teor. Fiz. 47, 1483 (1964) [Soviet Phys. JETP 20, 997 (1965)].

[12] A. Omont, J. Phys. (Paris) 26, 576 (1965).

[13] We use a system of units in which $\hbar = c = 1$.

[14] M. Crance and A. Omont, Compt. Rend. 269B, 1230 (1969).

PHYSICAL REVIEW A VOLUME 3, NUMBER 6 JUNE 1971

Nonrelativistic Auger Rates, X-Ray Rates, and Fluorescence Yields for the K Shell[*]

D. L. Walters and C. P. Bhalla
Department of Physics, Kansas State University, Manhattan, Kansas 66502
(Received 23 November 1970)

The Auger rates, x-ray rates, and fluorescence yields are presented for elements $Z = 4-54$ when a vacancy is in the K shell. Numerical calculations have been performed using the Hartree-Fock-Slater approach with Kohn-Sham and Gaspar exchange. Comparisons of different exchange approximations on the Auger and x-ray total transition rates and the fluorescence yields are reported. The differences are found to be $\approx 10-20\%$ at low Z and to decrease with increasing Z.

I. INTRODUCTION

There have been several nonrelativistic theoretical computations of the Auger transition rates.[1] Among these, a variety of atomic models have been utilized. The hydrogenic approximation has been used by Burhop,[2] Asaad and Burhop,[3] and quite extensively by Callan.[4] Rubenstein[5] has performed Hartree-Fock calculations for three elements: argon, krypton, and silver.

More recently, McGuire[6,7] has presented computations for 27 elements in the range $4 \leq Z \leq 54$ using the Hartree-Fock-Slater (HFS) model. Considerable local structure exists in the Z dependence of the K-LL Auger transition rates.[6,7] Generally, little structure would be expected in a process like the K-shell Auger effect which is predominantly concerned with core electrons. This would suggest that independent calculations be performed to verify whether the theoretical results of McGuire are correct. We have recently reported a brief summary of our independent calculations,[8] which shows no local structure in the K-LL Auger rates.

Theoretical relative intensities calculated with a pure coupling scheme such as L-S or J-J coupling do not generally compare very well with experiment. It is usually necessary to include configuration interaction and intermediate coupling in the interactions.[9,10] Regardless of the coupling scheme chosen, all such calculations require the same radial matrix elements. The accuracy of these matrix elements depends on the atomic model chosen. These matrix elements have not been available for a realistic atomic model.

The Hartree-Fock model would be preferable; however, the inherent complexity prohibits its use in extensive Auger calculations. The recent works of Slater *et al.*,[11] Herman, Van Dyke, and Ortenburger[12] (HVO), and others show that the HFS model can be made to yield wave functions essentially equivalent to the Hartree-Fock results (in terms of the total energy) when the proper exchange approximation is made. Folland[13] has shown that the Kohn and Sham[14] and Gaspar[15] (KSG) exchange approximation gives a free-electron exchange density which is quite close to the true Hartree-Fock exchange density, and that the HVO refinement is a justifiable improvement. No extensive comparison of the various approximations on the x-ray, Auger, and fluorescence yields has previously been attempted.

It is the purpose of this paper to present K-shell Auger matrix elements, Auger transition rates, x-ray transition rates, and fluorescence yields for all atoms from $Z=4$ to $Z=54$. We have employed the HFS model with the KSG exchange approximation. The effects of the exchange approximations on the various rates are also presented.

Section II contains the calculational procedure followed by the numerical results in Sec. III. A discussion and the conclusion are given in Sec. IV.

II. METHOD OF CALCULATION

We use atomic units throughout this paper ($e=m_e=\hbar=1$). The units for energy and time are 2 Ry (27.2 eV) and 2.43×10^{-17} sec, respectively.

A. Bound-State and Continuum Wave Functions

The bound-state radial wave functions were obtained from a nonrelativistic HFS program.[16] The exchange approximation used in this program has the form

$$V^{\text{exch}}(r) = -3\alpha\left[(3/8\pi)\left|\rho(r)\right|\right]^{1/3} . \qquad (1)$$

Slater exchange[17] corresponds to $\alpha=1$ and KSG exchange occurs when $\alpha=\frac{2}{3}$. Both the initial and final electron wave functions used in Auger and x-ray calculations were HFS solutions corresponding to an atom with an initial K-shell vacancy. The Latter[18] tail correction was used.

The continuum-electron solutions P_{kl} (described by the wave vector k and the angular momentum l) were determined by numerically solving

$$\left(\frac{d^2}{dr^2} - \frac{l(l+1)}{r^2} + 2\left[E - V(r)\right]\right) P_{kl}(r) = 0 . \qquad (2)$$

The potential $V(r)$ was the appropriate potential developed in the HFS solution for the bound electrons. A power-series expansion for P_{kl} was employed for small values of r and then Numerov integration was applied and continued until the solution had become quite asymptotic.

The asymptotic solution is known and, using energy normalization, is given by[19]

$$P_{kl}(r) \approx (2/\pi k)^{1/2} \cos\left[kr + 2k^{-1}\ln 2kr - \tfrac{1}{2}\pi(l+1) - \delta_l\right] . \qquad (3)$$

Using the derivative of (3) we can write

$$P_{kl}^2(r) + \frac{P_{kl}'^2(r)}{(1+2/kr)^2} = \frac{2}{\pi k} , \qquad (4)$$

which is true for all large r. Similarly, the numerical solution, Eq. (2), can be normalized by requiring Eqs. (3) and (4) to hold at large r. Also, since Eq. (4) is independent of r for large r, we have a convenient test for indicating when the numerical solutions have become asymptotic.

B. Auger Transitions

In order to calculate Auger transition rates $T(a\to b)$, we use the expression (in atomic units)

$$T_A(a\to b) = 2\pi\left|\langle b\,|\,(1/r_{ij})\,|a\rangle\right|^2 \rho_F , \qquad (5)$$

where ρ_F represents the density of final states which is equal to unity for energy normalization of the continuum-electron wave function.

The matrix element of Eq. (5) has an initial state (a) containing two bound-electron wave functions designated by n_1l_1 and n_2l_2. The final state (b) is composed of a bound-state wave function n_3l_3 and a continuum-electron wave function kl_4. The wave function may be separated into a radial part $P_{n_il_i}/r_i$ and an angular part $Y_{l_i}^{m_i}(\theta,\phi)$. Using antisymmetrized product wave functions, the matrix element in Eq. (5) can be written in $LSJM$ coupling in terms of 3-J and 6-J symbols by[20,21]

$$\langle b\,|1/r_{ij}|\,a\rangle=\tau(-1)^{L+l_1+l_4}\sum_{\kappa}\Bigg[R_\kappa(1,2,3,4)\langle l_3\|C^\kappa\|l_1\rangle\langle l_4\|C^\kappa\|l_2\rangle\begin{Bmatrix} l_3 & l_4 & L\\ l_2 & l_1 & \kappa\end{Bmatrix}$$

$$+(-)^{L+S}R_\kappa(1,2,4,3)\langle l_3\|C^\kappa\|l_2\rangle\langle l_4\|C^\kappa\|l_1\rangle\begin{Bmatrix} l_3 & l_2 & L\\ l_1 & l_2 & \kappa\end{Bmatrix}\Bigg]\,, \qquad (6a)$$

where

$$\langle l\|C^\kappa\|l'\rangle=[(2l+1)(2l'+1)]^{1/2}\begin{pmatrix} l' & \kappa & l\\ 0 & 0 & 0\end{pmatrix}(-1)^l\,, \qquad (6b)$$

$$R_\kappa(1,2,3,4)=\int_0^\infty\int_0^\infty P_{n_1l_1}(i)\,P_{n_2l_2}(j)\,(r_<^\kappa/r_>^{\kappa+1})\,P_{n_3l_3}(i)\,P_{\kappa l_4}(j)\,dr_i\,dr_j\quad. \qquad (6c)$$

In Eqs. (6), the angular and radial dependence have been separated. Both direct and exchange contributions occur. Normally, $\tau=1$, but if n_1l_1 and n_2l_2 are equivalent electrons, $\tau=\sqrt{\frac{1}{2}}$.

Since magnetic states are not normally observed, it is necessary to average Eq. (1) over the initial states and sum over the final states. For a particular J, one form for the Auger transition rate is then

$$T_A(a\rightarrow b)=\frac{2J+1}{2(2l_3+1)}\times 2\pi\,|\langle b\,|(1/r_{ij})|\,a\rangle|^2\quad. \qquad (7)$$

Equations (6) and (7) are equivalent to the expressions given by Asaad and Burhop[3] and are correct when the final vacancies (n_1l_1 and n_2l_2) are produced from closed shells. When this is not the case, the angular dependence becomes complex. If we are interested in the total Auger transition rate involv-

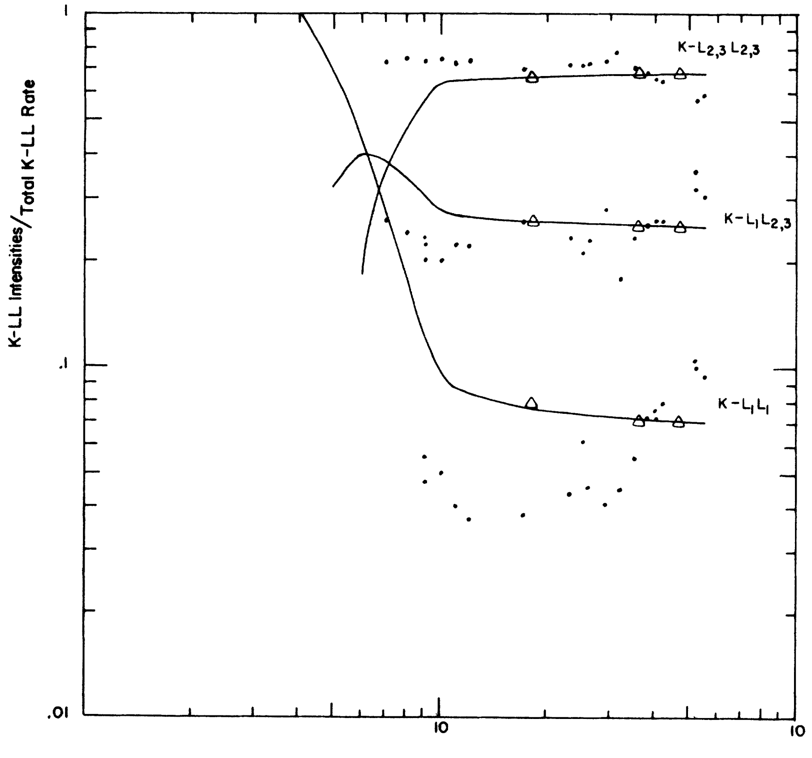

FIG. 1. Comparison of the theoretical K-LL intensities in the L-S coupling scheme with the experimental data (Refs. 25-45) versus atomic number (relative to the total K-LL transition rates). The solid lines represent the present results, the triangles indicate the calculations of Ref. 5, and the solid points are the experimental values. The results of Ref. 7 differ from the present by showing considerable structure (≈ 50%) in the K-L_1L_1 line.

TABLE I. Theoretical K-shell x-ray[a] and Auger rates per atomic time unit and K-shell fluorescence yield (W_K).

Z	X-ray rate	Auger rate (units of 10^{-2})	W_K
5	9.984 (−7)	0.1237	0.0008
6	4.864 (−6)	0.2059	0.0024
7	1.517 (−5)	0.3221	0.0047
8	3.686 (−5)	0.4777	0.0077
9	7.751 (−5)	0.6646	0.0115
10	1.475 (−4)	0.8869	0.0164
11	2.464 (−4)	1.076	0.0224
12	3.834 (−4)	1.234	0.0301
13	5.736 (−4)	1.384	0.0398
14	8.308 (−4)	1.532	0.0514
15	1.170 (−3)	1.676	0.0653
16	1.610 (−3)	1.807	0.0818
17	2.171 (−3)	1.945	0.1004
18	2.874 (−3)	2.079	0.1215
19	3.728 (−3)	2.201	0.1448
20	4.760 (−3)	2.311	0.1708
21	5.963 (−3)	2.399	0.1991
22	7.301 (−3)	2.482	0.2273
23	9.035 (−3)	2.561	0.2608
24	1.093 (−2)	2.626	0.2939
25	1.316 (−2)	2.701	0.3276
26	1.569 (−2)	2.760	0.3624
27	1.857 (−2)	2.812	0.3977
28	2.183 (−2)	2.860	0.4329
29	2.547 (−2)	2.898	0.4678
30	2.964 (−2)	2.948	0.5014
31	3.435 (−2)	3.000	0.5338
32	3.965 (−2)	3.053	0.5650
33	4.559 (−2)	3.107	0.5947
34	5.221 (−2)	3.160	0.6230
35	5.959 (−2)	3.211	0.6498
36	6.781 (−2)	3.260	0.6754
37	7.679 (−2)	3.306	0.6987
38	8.668 (−2)	3.351	0.7211
39	9.750 (−2)	3.393	0.7420
40	1.093 (−1)	3.433	0.7611
41	1.222 (−1)	3.472	0.7788
42	1.362 (−1)	3.510	0.7951
43	1.515 (−1)	3.571	0.8093
44	1.681 (−1)	3.599	0.8236
45	1.860 (−1)	3.625	0.8367
46	2.054 (−1)	3.650	0.8491
47	2.264 (−1)	3.674	0.8605
48	2.491 (−1)	3.698	0.8707
49	2.736 (−1)	3.721	0.8803
50	3.001 (−1)	3.745	0.8889
51	3.286 (−1)	3.768	0.8971
52	3.592 (−1)	3.793	0.9046
53	3.921 (−1)	3.816	0.9112
54	4.276 (−1)	3.844	0.9176

[a] The numbers in parentheses after an entry are the powers of 10 to be multiplied by it.

ing a nonfilled shell, simplifications occur.[22] When the final vacancies occur in different shells, and one of the shells initially has n electrons when it could have m, then the full shell rate is reduced by n/m. If the final vacancies are both in the same shell, the full-shell rate is reduced by $n(n-1)/m(m-1)$.

The Auger electron energies E were found by subtracting the appropriate electron binding energies obtained from the HFS neutral atom calculations (with Slater exchange). These calculated Auger electron energies generally agree ($\leq 0.5\%$) with the experimentally measured energies. The effect of such an error in the Auger electron energies on the transition rates is of similar magnitude.

The radial integrals in Eqs. (6) were computed using five-point Newton-Codes quadrature. The three bound-state wave functions were first converted to the continuum wave function mesh by using Lagrange interpolation. The integration was continued until one of the bound wave functions reached its practical infinity.

C. X-Ray Transitions

The total x-ray transition rate in the electric dipole approximation for an initial vacancy n_il_i and a final vacancy n_fl_f is given in atomic units by

$$T_x(i\to f)=\tfrac{4}{3}k^3\,\frac{l_>}{2l_i+1}\left|\int_0^\infty P_{n_il_i}\,P_{n_fl_f}\,r\,dr\right|^2 , \qquad (8)$$

where $l_>$ is the greater of l_i and l_f.

The magnitude of the x-ray wave vector k is determined from the electron binding energies, $k=(E_i-E_f)/c$. Two bound-state radial wave functions $P_{n_il_i}$ and $P_{n_fl_f}$ occur in the radial integral of Eq. (8). The x-ray intensities depend strongly on k, we therefore used the experimentally measured energies of Bearden and Burr[23] in calculating k. If the shell in which the final vacancy n_fl_f occurs is not full but contains m electrons when it could hold m_0, the full-shell rate is reduced by m/m_0.

D. Fluorescence Yield

The K-shell fluorescence yield W_K is calculated from the total K-shell x-ray rate T_x and the total K-shell Auger transition rate T_A:

$$W_K=T_x/(T_x+T_A) \ . \qquad (9)$$

III. NUMERICAL RESULTS

The Auger and the x-ray transition rates were calculated with the HFS model, as described in Sec. II. The KSG exchange approximation was used for every Z. All the present calculations correspond to a single K-shell vacancy.

The K-shell Auger radial matrix elements and transition rates for the K-LL, K-LM_1, K-$LM_{2,3}$, and the K-$M_{1,2,3}\,M_{1,2,3}$ transitions are presented elsewhere.[24] The radial matrix elements are defined in Eq. (6). Energy normalization of the Auger electron has been used. The transition rates are

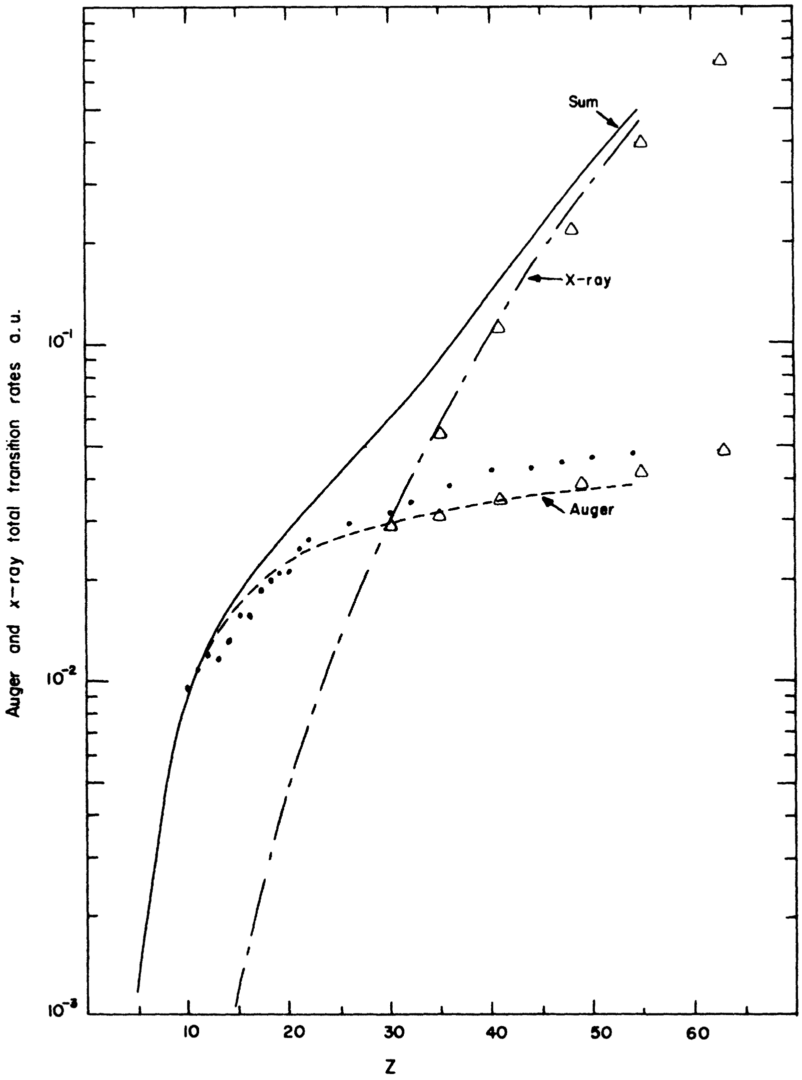

FIG. 2. Nonrelativistic total K-shell x-ray and Auger transition rates and their sums versus atomic number. The triangles indicate the relativistic results of Refs. 46 and 47, and the solid points represent the calculations of Ref. 7.

in atomic time units. Table I contains the total x-ray and total Auger transition rates along with the calculated fluorescence yields.

In Fig. 1, the K-LL intensities, relative to the total K-LL transition rates (in the L-S coupling scheme), are compared with the experimental data. The total x-ray and Auger transition rates are plotted as a function of Z in Fig. 2. We have included for comparison the relativistic HFS results of Bhalla and Ramsdale,[46] Rosner and Bhalla,[47] and the nonrelativistic Auger rates of McGuire.[7] In Fig. 3, the fluorescence yields are presented along with the experimental values.[48,49]

The effects of different exchange approximations used in the HFS model on the x-ray and Auger total transition rates and on the fluorescence yields were calculated. In Fig. 4, the results for Slater exchange ($\alpha = 1$) are compared with those for KSG exchange ($\alpha = \frac{2}{3}$). Relative to the KSG results, Slater exchange increases the Auger and the x-ray yields while decreasing the fluorescence yields.

Herman, Van Dyke, and Ortenburger (HVO)[12] have included an inhomogenity term in the free-electron exchange approximation. In the notation of HVO, we have performed calculations using $\alpha = \frac{2}{3}$ and $\beta = 0.004$. Figure 5 compares computations for the HVO exchange to those with KSG exchange. Relative to the KSG exchange results, HVO exchange decreases all three yields.

IV. DISCUSSION AND CONCLUSION

It is convenient to separate the discussion into two sections. Section IV A is concerned with the results for $Z < 10$, and Sec. IV B considers $Z \geq 10$.

A. Low Z (< 10)

For $Z < 10$, the L shells ($2p$) are being filled.

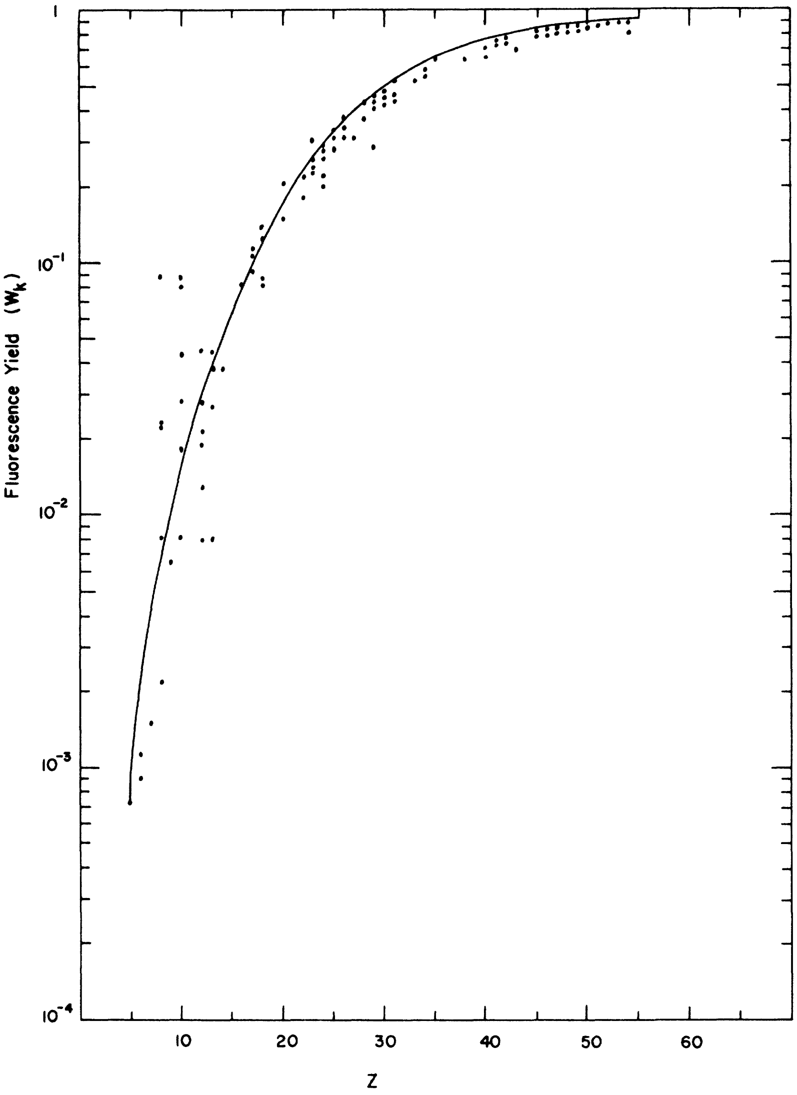

FIG. 3. Comparison of the theoretical K-shell fluorescence yield W_K (solid line) with the experimental data (Refs. 48 and 49) versus atomic number.

This accounts for the structure in the K-LL relative intensities. Comparison with experiment is difficult since these electrons are involved in chemical bonds of the solids used in most measurements. The theoretical transition rates are for free atoms, and such chemical effects would be expected to have an influence on the experimental results.

Some comparisons can be made for the fluorescence yields. The theoretical fluorescence yields are generally larger (≈ 50%) than the experimental values. These measurements[49] were made on solids and it appears that the chemical bonding reduces the x-ray transition rates more than the corresponding Auger rates. The theoretical results of McGuire are similar to the present although they are about 20–30% larger.

The choice of exchange approximation has a very pronounced effect on the theoretical calculations for $Z < 10$. The Slater exchange leads to Auger transition rates 15–25% larger than the KSG exchange. The x-ray rates are also larger by 5–10%. The fluorescence yield is reduced by 9–14% as compared to the results for KSG exchange.

The difference between KSG and HVO exchange is also rather pronounced, especially for very low Z. The x-ray rates are affected the most and are smaller than the KSG results by 4–15%. The Auger rates are decreased by 2–9%, while the fluorescence yields are lowered by 1–7%.

B. Moderate Z ($10 \leqslant Z \leqslant 54$)

With the L shells filled, the theoretical relative intensities change smoothly with increasing Z. The hydrogenic results of Callan show the same behavior, but McGuire reports some structure, especially in the K-L_1L_1 line. The agreement of

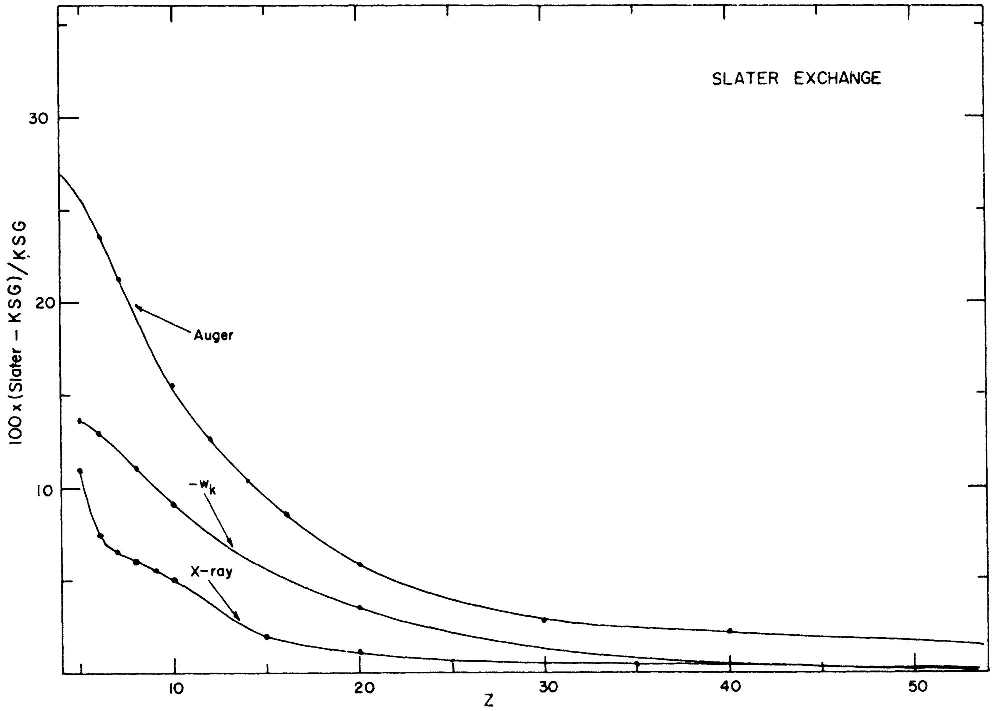

FIG. 4. Percentage difference between the theoretical results using Slater exchange ($\alpha = 1$) and those with KSG exchange ($\alpha = \frac{2}{3}$) versus atomic number. Comparisons are made for the total Auger and x-ray transition rates and the fluorescence yields.

the present results with the Hartree-Fock calculations of Rubenstein is excellent.

Comparison of relative intensities with experiment is complicated by configuration interaction. The K-L_1L_1 ($^1S_0$) transition is strongly perturbed by the K-L_2L_2 ($^1S_0$) transition, as has been demonstrated by the semiempirical calculations of Asaad.[9,10] The effect of this interaction is to in-

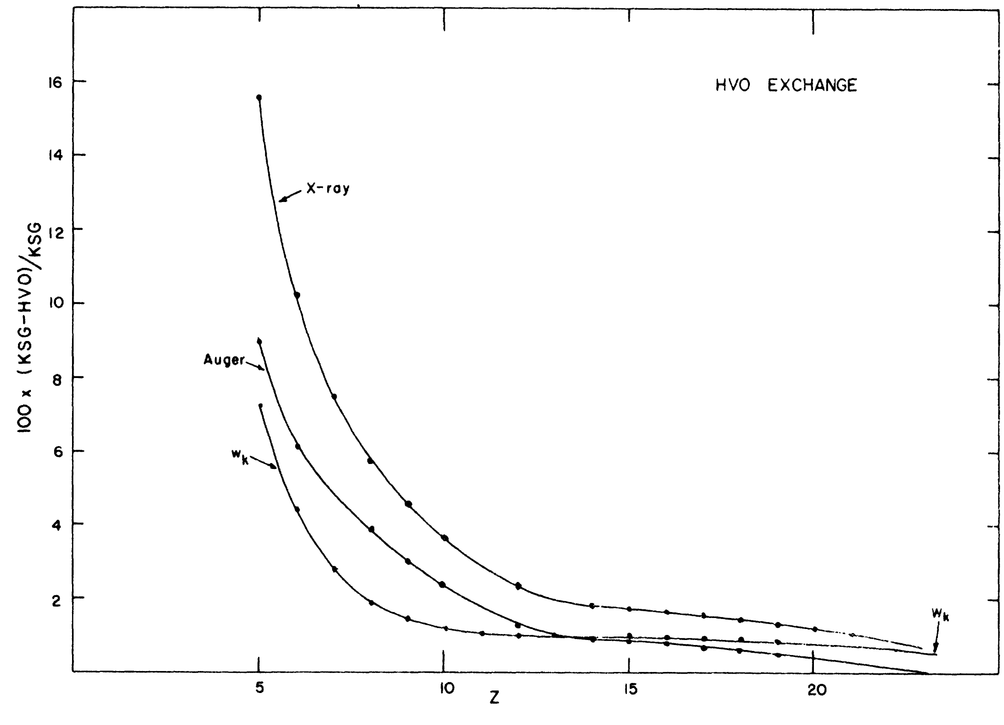

FIG. 5. Percentage difference between the theoretical results using HVO exchange ($\alpha = \frac{2}{3}$, $\beta = 0.004$) and those with KSG exchange ($\alpha = \frac{2}{3}$) versus atomic number. Comparisons are made for the total Auger and x-ray transition rates and the fluorescence yields.

crease the K-L_2L_2 intensity at the expense of the K-L_1L_1 line. Configuration interaction appears to be predominant in the region $10 < Z < 25$. Nevertheless, the agreement of the present relative intensities and experiment improves and is excellent for $Z = 38$. At higher atomic numbers, the L-S coupling becomes inadequate and relativistic effects become important.

In the present calculations the total Auger transition rates increases very smoothly with increasing Z. The agreement with the results of Rubenstein are ($\approx 2\%$) for $Z = 36$ and 47. Rubenstein predicts a rate 20% lower for $Z = 18$; however, this is probably a result of computational errors: "There is evidence that we have overestimated the effects of screening in argon."[5] The agreement with McGuire is rather poor. The results of McGuire show considerable fluctuations vs Z, and for higher Z these calculations differ from the present by $\approx 22\%$. The total x-ray transition rates of McGuire are larger than the present by 20% ($Z = 10$). This difference slowly decreases to $\approx 4\%$ ($Z = 54$).

The agreement of the Auger rates with the relativistic results[46,47] is good ($\approx 3\%$). The nonrelativistic total x-ray rates are larger than those predicted relativistically, especially for high Z ($\approx 12\%$). This probably results from the neglect of retardation in the nonrelativistic calculations.

Up to about $Z = 40$, the theoretical fluorescence yields agree to within the limits of uncertainty for most of the experimental values (especially for those measurements with small experimental uncertainties[48]). For higher Z, relativistic effects become significant. This is primarily the result of the overestimation in the x-ray rates. The agreement of the fluorescence yields with those of McGuire ranges from $\approx 12\%$ ($Z = 10$) to 1% ($Z = 54$). This agreement for high Z is somewhat surprising considering the large discrepancy in the Auger rates.

The choice of exchange approximations has less influence on the calculations for these atomic numbers. The K-LL relative intensities are quite insensitive to the differences in exchange. Both the Slater and the HVO exchange approximations result in relative intensities which differ from the KSG results by less than 5% for neon and the difference becomes small ($< 0.5\%$) at large Z.

The Auger rates with the Slater exchange approximation are larger than those for the KSG exchange and the differences range from 15 to 2% with increasing Z. Also, for Slater exchange, the differences in the fluorescence yields and the x-ray rates decline from 9 and 5%, respectively, to about 0.3% for both yields. The results for HVO and KSG exchange are very similar and the differences become negligible at high Z: $\approx 4\%$ ($Z = 10$)–$\approx 0.2\%$ ($Z = 54$).

From independent evidence,[11-13] the HVO exchange approximation should be preferred. However, there is little difference between the HVO results and those for the KSG exchange except at very low Z. It is questionable whether the HVO scheme or even the HFS process is applicable for such low-Z (< 10) atomic systems. It is possible that the small differences resulting from the choice of exchange approximation could have a significant effect on configuration-interaction and intermediate-coupling calculations.

In conclusion we note that the nonrelativistic K-LL relative intensities and the K-shell Auger, x-ray, and fluorescence yields show very little structure with Z. The theoretical fluorescence yields agree with experiment except at very-low-Z values (< 10) and at high Z (> 40) where additional effects become important. The choice of exchange approximation in the HFS model has a significant effect on the calculations for low Z and becomes less important for high Z. We believe that the results presented[24] with the KSG exchange provide an accurate, consistent set of radial matrix elements for the K-shell Auger process.

ACKNOWLEDGMENT

One of us (DLW) would like to thank Dr. N. O. Folland for many helpful discussions concerning exchange approximations.

---

*Based, in part, on a dissertation to be submitted by D. L. Walters in partial fulfillment of the requirements for the degree of Doctor of Philosophy at Kansas State University.

[1] P. Auger, J. Phys. Radium 6, 205 (1925).

[2] E. H. S. Burhop, Proc. Roy. Soc. (London) 148, A272 (1934).

[3] W. N. Asaad and E. H. S. Burhop, Proc. Roy. Soc. (London) 71, 369 (1958).

[4] E. J. Callan, Phys. Rev. 124, 793 (1961).

[5] R. A. Rubenstein, Ph. D. thesis (University of Illinois, 1955) (unpublished).

[6] E. J. McGuire, Phys. Rev. 185, 1 (1969).

[7] E. J. McGuire, Phys. Rev. 2, A273 (1970).

[8] D. L. Walters and C. P. Bhalla, Phys. Rev. A 3, 519 (1971).

[9] W. N. Asaad, Nucl. Phys. 44, 399 (1963).

[10] W. N. Asaad, Nucl. Phys. 66, 494 (1964).

[11] J. C. Slater, T. M. Martin, and J. H. Wood, Phys. Rev. 179, 28 (1969).

[12] F. Herman, J. P. Van Dyke, and I. B. Ortenburger, Phys. Rev. Letters 22, 807 (1969).

[13] N. O. Folland, Phys. Rev. A 3, 1537 (1971).

[14] W. Kohn and L. J. Sham, Phys. Rev. 140, A1133 (1965).

[15] R. Gaspar, Acta Phys. Acad. Sci. Hung. 3, 263 (1954).

[16] F. Herman and S. Skillman, *Atomic Structure Calcu-*

lations (Prentice-Hall, Englewood Cliffs, N. J., 1963).

[17] J. C. Slater, Phys. Rev. 81, 385 (1951).

[18] R. Latter, Phys. Rev. 99, 510 (1955).

[19] H. A. Bethe and E. E. Salpeter, *Quantum Mechanics of One- and Two-Electron Atoms* (Academic, New York, 1957).

[20] B. W. Shore and D. H. Menzel, *Principles of Atomic Spectra* (Wiley, New York, 1968).

[21] A. de-Shalit and I. Talmi, *Nuclear Shell Theory* (Academic, New York, 1963).

[22] E. J. McGuire, Sandia Research Report No. SC-RR-69-137, 1969 (unpublished).

[23] J. A. Bearden and A. F. Burr, Rev. Mod. Phys. 39, 125 (1967).

[24] Copies are available from the authors; also (unpublished).

[25] W. Mehlhorn, Z. Physik 160, 247 (1960).

[26] R. G. Albridge, K. Hamren, G. Johansson, and A. Fahlman, Z. Physik 209, 419 (1968).

[27] H. Körber and W. Mehlhorn, Z. Physik 191, 217 (1966).

[28] A. Fahlman, R. Nordberg, C. Nordling, and K. Siegbahn, Z. Physik 192, 476 (1966).

[29] B. Cleff and W. Mehlhorn, Z. Physik 219, 311 (1969).

[30] W. Mehlhorn and R. G. Albridge, Z. Physik 175, 506 (1963).

[31] J. Bellicard and A. Moussa, J. Phys. Radium 7, 115 (1957).

[32] Y. Y. Lui and R. G. Albridge, Nucl. Phys. A92, 139 (1967).

[33] J. Bellicard, Nucl. Phys. 3, 307 (1957).

[34] E. Sokolowski and C. Nordling, Arkiv Fysik 14, 557 (1959).

[35] M. S. Freedman, F. T. Porter, and F. Wagner, Phys. Rev. 151, 886 (1966).

[36] I. Bergström, Y. Y. Chu, and G. T. Emergy, Nucl. Phys. 62, 401 (1965).

[37] R. E. Johnson, J. H. Douglas, and R. G. Albridge, Nucl. Phys. A91, 505 (1967).

[38] P. Erman, I. Bergström, Y. Y. Chu, and G. T. Emergy, Nucl. Phys. 62, 401 (1965).

[39] O. Hörnfledt, A. Fahlman, and C. Nordling, Arkiv Fysik 23, 155 (1962).

[40] F. A. Johnson and J. S. Foster, Can. J. Phys. 31, 469 (1959).

[41] R. J. Krisciokaitis and S. K. Haynes, Nucl. Phys. A104, 466 (1967).

[42] W. R. Casey and R. G. Albridge, Z. Physik 219, 216 (1969).

[43] R. L. Graham, I. Bergström, and F. Brown, Nucl. Phys. A39, 107 (1962).

[44] P. Erman and Z. Sujkowski, Arkiv Fysik 20, 209 (1961).

[45] R. L. Graham, F. Brown, G. T. Ewan, and J. Uher, Can. J. Phys. 38, (1961).

[46] C. P. Bhalla and D. J. Ramsdale, Z. Physik 239, 95 (1970).

[47] H. R. Rosner and C. P. Bhalla, Z. Physik 231, 347 (1970).

[48] R. W. Fink, R. C. Jopson, Hans Mark, and C. D. Swift, Rev. Mod. Phys. 38, 513 (1966).

[49] C. E. Dick and A. C. Lucas, Phys. Rev. A 2, 580 (1970).

PHYSICAL REVIEW A VOLUME 3, NUMBER 6 JUNE 1971

Low-Velocity Moderation of Σ^- Hyperons in Hydrogen[†]

H. A. Rubin, R. A. Burnstein, and R. C. Misra*
Illinois Institute of Technology, Chicago, Illinois 60616

(Received 21 September 1970)

A measurement of the low-velocity moderation of Σ^- hyperons in hydrogen has been performed in a bubble-chamber experiment. The technique employed determines very accurately the Σ^- velocity at decay, $\Delta\beta = \pm 0.004$, by using $\Sigma^- \rightarrow \pi^- + n$ decays accompanied by neutron scatters with visible proton recoils. The results of the study, based on 23 200 Σ^- leading to 151 events with recoils in the region $\beta_{\Sigma^-} < 0.10$, indicate that the Σ^- moderation time for $\beta > 0.02$ agrees with the predictions of energy-loss theory using the first-order Born approximation and with experimental energy-loss data for protons. However, for the region $0.01 < \beta < 0.02$, the moderation-time data for Σ^- (and π^-) in hydrogen no longer agree with calculations based on the Born approximation or with experimental data for protons. The results for hydrogen are discussed and interpreted as being related to an "excess-range" effect previously observed for negative particles in emulsion.

I. INTRODUCTION AND BACKGROUND

This paper is a description of a study of the low-velocity moderation of charged particles in a region where there have been few experimental data. The theoretical treatment of the energy-loss phenomena of charged particles in matter originated with the work of Bethe,[1] which resulted in a Born-approximation expression for the energy loss per unit path length

$$-\frac{dE}{dx} = \frac{4\pi z^2 e^4}{mv^2} NZ \ln\left(\frac{2mv^2}{I}\right). \tag{1}$$

In this expression, ez is the charge of the incident particle, v is its velocity, m is the electron mass, Z and N are the atomic number and density of the